

Measurement of the Charge Number Per Adsorbed Molecule and Packing Densities of Self-Assembled Long-Chain Monolayers of Thiols

Thamara Laredo,[†] Jay Leitch,[†] Maohui Chen,[†] Ian J. Burgess,^{†,§} John R. Dutcher,[‡] and Jacek Lipkowski^{*,†}

Department of Chemistry, University of Guelph, Guelph, Ontario, N1G 2W1, Canada, and Department of Physics, University of Guelph, Guelph, Ontario, N1G 2W1, Canada

Received January 23, 2007

We have applied a recently developed method (*Langmuir* 2006, 22, 5509–5519) to determine charge numbers per adsorbed molecule and packing densities in self-assembled monolayers (SAMs) of octadecanethiol (C₁₈SH), a representative long-chain thiol. Our method yields values of area per molecule that are physically reasonable, in contrast to the popular reductive desorption method, which gives molecular areas that are smaller than those determined by the van der Waals radii. In a nonadsorbing electrolyte, we were able to model the dependence of the charge number per adsorbed molecule on the electrode potential, taking into account that the desorption process is a substitution reaction between the solvent and the adsorbate. We have also shown that the charge number per adsorbed thiol is affected by the specific adsorption of the anion of the electrolyte. In the latter case, the thiol competes for adsorption sites at the surface not only with water but also with the anion of the electrolyte, and this competition has an effect on the measured charge number.

Introduction

The accurate determination of the composition, quality, and coverage of self-assembled monolayers (SAMs) is tremendously important for their application in devices such as biosensors.^{2,3} Various methodologies have been employed for this purpose including vibrational spectroscopy,^{4,5,6} quantitative X-ray photoelectron spectroscopy,⁷ and scanning probe microscopy.^{8,9} Electrochemical characterization of SAMs composed of thiolate–Au linkages is particularly appealing due to its ease of application and its sensitivity to the integrity of the film. For example, the presence of a redox couple in the electrolyte gives rise to a voltammetric signal that can be used as a measure of the film's pinhole defect density.^{10–13} If the thiol itself contains a redox center, such as ferrocene, electrochemical determination of the surface coverage of the SAM can be achieved by integration of the voltammetric signal.¹⁴

In the case of redox-inactive SAMs, the commonly accepted means to determine the surface coverage is to cathodically desorb the monolayer.^{15–17} Integration of the current corresponding to the reductive desorption peak, between the potential at which the monolayer is adsorbed, E_a , and a sufficiently negative potential at which the monolayer is desorbed, E_d , yields the total charge of the thiolate desorption process:

$$Q = \int_{E_a}^{E_d} \frac{i}{v} dE \quad (1)$$

where v is the voltage sweep rate. It is assumed that an integer number of n electrons (in the case of simple thiolates, $n = 1$)¹⁵ is consumed by one adsorbed thiol(ate) as described by the reaction



where the terms in parentheses, (s), (Au), and (aq) refer to the metal's surface, the bulk gold phase, and the solution phase, respectively. The monolayer coverage, Γ , is then obtained from the Faraday Law:

$$\Gamma = \left| \frac{Q}{nF} \right| \quad (3)$$

where F is Faraday's constant. It is widely believed that the value of charge, Q , measured in this fashion provides an accurate measurement of the monolayer coverage if the reductive voltammetry is performed in an electrolyte sufficiently basic to prevent concomitant hydrogen evolution.

The approach described above is flawed on two accounts. First, in eq 1 the integrand is equal to the differential capacity

* To whom correspondence should be addressed. E-mail: jlipkows@uoguelph.ca.

[†] Department of Chemistry.

[‡] Department of Physics.

[§] Current Address: Department of Chemistry, University of Saskatchewan, Saskatoon, Saskatchewan, S7N 5C9, Canada.

(1) Kunze, J.; Leitch, J.; Schwan, A. L.; Faragher, R. J.; Naumann, R.; Schiller, S.; Knoll, W.; Dutcher, J. R.; Lipkowski, J. *Langmuir* 2006, 22, 5509–5519.

(2) Xu, Y.; Kraatz, H. B. *Tetrahedron Lett.* 2001, 42, 2601–2603.

(3) Willner, I.; Katz, E.; Willner, B.; Blonder, R.; Heleg-Shabtai, V.; Buckmann, A. F. *Biosens. Bioelectron.* 1997, 12, 337–356.

(4) Parikh, A. N.; Allara, D. L. *J. Chem. Phys.* 1992, 96, 927–945.

(5) Dannenberger, O.; Buck, M.; Grunze, M. *J. Phys. Chem. B* 1999, 103, 2202–2213.

(6) Yeganeh, M. S.; Dougal, S. M.; Polizzotti, R. S.; Rabinowitz, P. *Phys. Rev. Lett.* 1995, 74, 1811–1814.

(7) Dannenberger, O.; Weiss, K.; Himmel, H.-J.; Jager, B.; Buck, M.; Woll, C. *Thin Solid Films* 1997, 307, 183–191.

(8) Poirier, G. E. *Chem. Rev.* 1997, 97, 1117–1128.

(9) Liu, G.-Y.; Fenter, P.; Chidsey, C. E. D.; Ogletree, D. F.; Eisenberger, P.; Salmeron, M. *J. Chem. Phys.* 1994, 101, 4301–4306.

(10) Porter, M. D.; Bright, T. B.; Allara, D. L.; Chidsey, C. E. D. *J. Am. Chem. Soc.* 1987, 109, 3559–3568.

(11) Bizzotto, D.; McAlees, A.; Lipkowski, J.; McCrindle, R. *Langmuir* 1995, 11, 3243–3250.

(12) Ma, F.; Lennox, R. B. *Langmuir* 2000, 16, 6188–6190.

(13) Finklea, H. O.; Snider, D. A.; Fedyk, J.; Sabatini, E.; Gafni, Y.; Rubinstein, I. *Langmuir* 1993, 9, 3660–3667.

(14) Lindholm-Sethson, B.; Orr, J. T.; Majda, M. *Langmuir* 1993, 9, 2161–2167.

(15) Widrig, C. A.; Chung, C.; Porter, M. D. *J. Electroanal. Chem.* 1991, 310, 335–359.

(16) Walczak, M. M.; Popenoe, D. D.; Deinhammer, R. S.; Lamp, B. D.; Chung, C.; Porter, M. D. *Langmuir* 1991, 7, 2687–2693.

(17) Kakiuchi, T.; Ususi, H.; Hobara, D.; Yamamoto, M. *Langmuir* 2002, 18, 5231–5238.

($i/v = C$), which for a thiol covered electrode is described by¹⁸

$$C = C_{\infty} + \left(\frac{\partial \sigma_M}{\partial \Gamma} \right)_E \frac{d\Gamma}{dE} \quad (4)$$

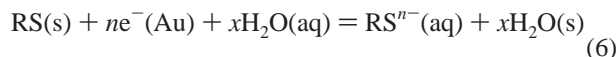
where $(\partial \sigma_M / \partial \Gamma)_E = -lF$, C_{∞} is the true or infinite frequency capacity and l is the formal charge number at a constant potential, known also as the electrosorption valency,¹⁹ which cannot be assumed to be independent of potential. Therefore, the integral of the voltammetric current corresponding to the cathodic desorption of the thiol is equal to

$$Q = \int_{E_a}^{E_d} \frac{i}{v} dE = \int_{E_a}^{E_d} C_{\infty} dE - F \int_{\Gamma}^0 l d\Gamma \quad (5)$$

It is apparent that eqs 3 and 5 are equal provided $\int_{E_a}^{E_d} C_{\infty} dE = 0$ and $|l| = n$.

The term $\int_{E_a}^{E_d} C_{\infty} dE$ (known also as the double-layer charging term) is never equal to zero. As a consequence, the reductive desorption method leads to packing densities that are systematically too high and corresponding molecular areas that are too small. The pitfalls of neglecting the contribution of the double-layer charging to the total charge of desorption were highlighted by Schneider and Buttry nearly 15 years ago.²⁰ In the interim, efforts have been made to account for double-layer charging effects in chronoamperometric,²¹ cyclic,²² and linear sweep voltammetric²³ studies of reductive thiol desorption. However, these studies remain the exceptions to the common practice of neglecting the $\int_{E_a}^{E_d} C_{\infty} dE = 0$ term.

The second problem with the cathodic desorption method is that $|l| \neq n$. This was shown by Krysinski et al.²⁴ who in an elegant experiment on octadecanethiol adsorption demonstrated that l is a partial charge number and is highly dependent on the electrode's potential. It was further pointed out by Schneider and Buttry,²⁰ that the charge number, l , does not need to be an integer. Recently, Kunze et al.¹ demonstrated that reaction 1 is oversimplified. In reality, the desorption process is a substitution reaction between the adsorbed thiol molecules and water from the bulk described by



and due to the water substitution nature of this reaction, the value of $|l|$ changes as a function of the applied potential from 0 to n .

Kunze et al.¹ developed a new method to determine the surface coverage of a self-assembled thiol. The method involves two measurements. First, a monolayer of the thiol of interest is transferred from the air/water interface to the Au(111) surface at a fixed surface pressure using the Langmuir–Blodgett (LB) technique. The measurement of the transfer ratio allows accurate determination of the packing density of the transferred monolayer. Chronocoulometric experiments are then performed to determine the charge density at the electrode in the presence of the adsorbed thiol. The electrosorption valency is determined from

$$l = - \frac{1}{F} \left(\frac{\Delta \sigma_M}{\Delta \Gamma} \right)_E \quad (7)$$

which is an integral form of the formal charge number defined

(18) Frumkin, A. N.; Damaskin, B. B. In *Modern Aspects of Electrochemistry*; Bockris, J. O. M., Conway, B. E., Eds.; Butterworths: London, 1964; Vol. 3, p 149

(19) Trasatti, S.; Parsons, R. *J. Electroanal. Chem.* **1986**, *205*, 359–376.

(20) Schneider, T. W.; Buttry, D. A. *J. Am. Chem. Soc.* **1993**, *115*, 12391–12397.

earlier. In a second experiment, the monolayer of thiol is self-assembled at the Au electrode surface. The values of l determined for the LB monolayer are assumed to be the same for the SAM. The chronocoulometric measurements for the electrode covered by the self-assembled film are then performed and the packing densities of the SAM are calculated from the measured charge densities.

Kunze et al.¹ applied the new method to determine packing densities for a Au(111) electrode covered by 2,3-di-phytanyl-*sn*-glycerol-1-tetraethylene glycol-DL-*a*-lipoic acid ester lipid (DPTL), which is quite a complex dithiolipid. A referee of that paper suggested that the methodology outlined above should be tested on a simple molecule such as an alkane thiol in order to generalize the results. In this manuscript, we apply the new method to determine the packing density for a monolayer of *n*-octadecanethiol (C₁₈SH) adsorbed at a Au(111) electrode surface, in response to this suggestion. C₁₈SH SAMs have been very well studied in the past^{24–26} making it an ideal molecule to test the method described by Kunze et al. We demonstrate that indeed $|l|$ changes from 0 to $\sim n$ as a function of the electrode potential. We also show that using the potential dependent values of l , one can determine physically reasonable packing densities for the SAM of C₁₈SH, in contrast to packing densities calculated using the reductive desorption method that are physically unrealistic.

Experimental Section

Reagents, Solutions, and Electrode Materials. Gold single crystals, prepared as described in ref 27 were used as working electrodes for electrochemistry measurements. Before each experiment, the working electrode was flame-annealed, cooled first in air, and then transferred into the electrochemical cell to cool further in an argon atmosphere. A flame-annealed gold coil was used as the counter electrode in all experiments. The reference electrode was an external saturated calomel electrode (SCE). In this paper, all potentials are referred to the SCE. The glassware was cleaned in acid (1:3 mixture of HNO₃ and H₂SO₄) and thoroughly rinsed with Milli-Q and Milli-Q UV plus water (Millipore, Bedford, MA), resistivity 18.2 MΩ cm. The electrochemical cell was soaked in Milli-Q water overnight and rinsed again prior to the experiment.

Either a 0.1 M NaOH (Aldrich, 99.99% semiconductor grade) solution or 0.1 KClO₄ (Aldrich, recrystallized as in ref 27) were used as the supporting electrolytes. The Milli-Q UV plus water was used to prepare the solutions. Before the experiment, electrolyte solutions were deaerated by purging with argon (BOC Gases, Mississauga, Ontario, Canada) for at least 40 min, and an argon blanket was maintained over the solution throughout the experiment. C₁₈SH (Aldrich, 98%) was dissolved in methanol and deposited onto the Au(111) surface by self-assembly. The self-assembly time was 24 h. This was long enough to form well-ordered monolayers. After formation of the SAM, the electrodes were rinsed with methanol and water before introduction to the electrochemical cell.

For the LB deposition, a few drops of C₁₈SH solution in chloroform were injected onto the water surface of the Langmuir trough. The solvent was allowed to evaporate, and then the compression isotherm was recorded. LB deposition was achieved by vertically withdrawing the electrode at a speed of 35 mm min⁻¹ at a constant transfer pressure of 10 mN m⁻¹. The transfer ratio was 1.0 ± 0.1. The trough was controlled by a computer using KSV LB5000 software. All transfers were carried out at a temperature of 27 ± 1 °C.

(21) Yang, D. F.; Wilde, C. P.; Morin, M. *Langmuir* **1997**, *13*, 243–249.

(22) Tadini Bounuinsegni, F.; Becucci, L.; Moncelli, M. R.; Guidelli, R. *J. Electroanal. Chem.* **2001**, *500*, 395–407.

(23) Kawaguchi, T.; Yasuda, H.; Shimazu, K.; Porter, M. D. *Langmuir* **2000**, *16*, 9830–9840.

(24) Krysinski, P.; Chamberlain, R. V.; Majda, M. *Langmuir* **1994**, *10*, 4286–4294.

(25) Schreiber, F. *Prog. Surf. Sci.* **2000**, *65*, 151–257.

(26) Bilewicz, R.; Majda, M. *Langmuir* **1991**, *7*, 2794–2802.

(27) Richer, J.; Lipkowski, J. *J. Electrochem. Soc.* **1986**, *133*, 121–128.

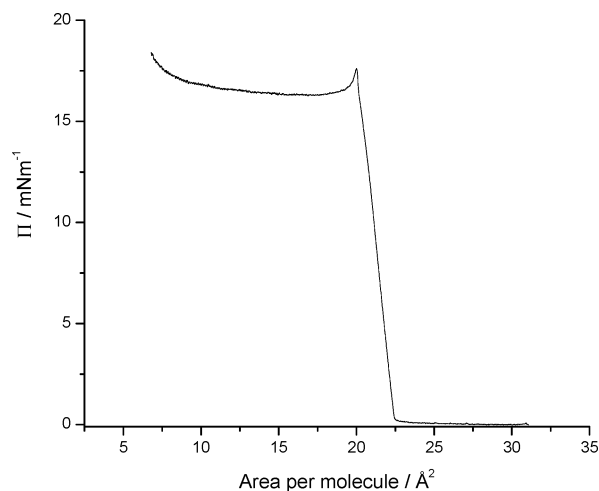


Figure 1. Compression isotherm for $C_{18}SH$ on a pure water subphase recorded at a compression rate of 10 mm min^{-1} .

Electrochemical Measurements and Instrumentation. Electrochemical measurements were carried out in an all-glass, three-electrode cell using the working electrode in the hanging meniscus configuration.^{27,28} Differential capacitance measurements were used to check the cleanliness of the electrode and the electrolyte solution. To determine the differential capacitance curves, an ac perturbation of 25 Hz frequency and 5 mV rms amplitude was superimposed onto a 5 mV s^{-1} voltage ramp. Electrochemical experiments were performed using a computer-controlled system, consisting of a HEKA potentiostat/galvanostat PG590, (HEKA, Lambrecht/Pfalz, Germany) and a 7265 DSP lock-in amplifier (EG&G Instruments, Cypress, CA). Data acquisition was performed via a plug-in acquisition board (NI-6052E, National Instruments, Austin, TX) and in-house software. A series RC equivalent circuit was employed to calculate the differential capacity curves from the in-phase and the out-of-phase components of the ac current.

In addition, chronocoulometry was employed to determine the charge density at the electrode surface. In this series of experiments, the Au(111) electrode was held at a base potential $E_{\text{base}} = -800 \text{ mV}$ for 300 s. Then the potential was stepped to a variable value, E_a , and kept at this potential for another 300 s. To desorb the thiol from the electrode surface, the potential was stepped from E_a to $E_{\text{des}} = -1400 \text{ mV}$. The current transient corresponding to the desorption of $C_{18}SH$ was measured over 0.4 s. The potential was then stepped back to the base value of $E_{\text{base}} = -800 \text{ mV}$. Integration of the current transients gives the difference between charge densities at potentials E_a and E_{des} . The charge density curves measured with and without $C_{18}SH$ merged at the most negative potentials. The absolute charge densities for the film free electrode can be calculated knowing the potential of zero charge, $E_{\text{pzc}} = 270 \text{ mV}$ versus SCE in 5 mM $KClO_4$ solution, determined independently. The data processing is described in detail in ref 29. The SAM was formed on the Au(111) electrode prior to each experiment.

Results and Discussion

$C_{18}SH$ Monolayer. Figure 1 depicts the surface pressure (Π)–molecular area isotherm for $C_{18}SH$ at the air/water interface. The shape of the compression isotherm is typical for a gel-like film in which the surface pressure increases very quickly with decreasing area per molecule. Compression starts at $\sim 23 \text{ \AA}^2$ per molecule with a collapse of the film occurring at a molecular area of $\sim 20 \text{ \AA}^2$ and a film pressure of 17 mN m^{-1} . This result agrees well with the work of Bilewicz and Majda.²⁶

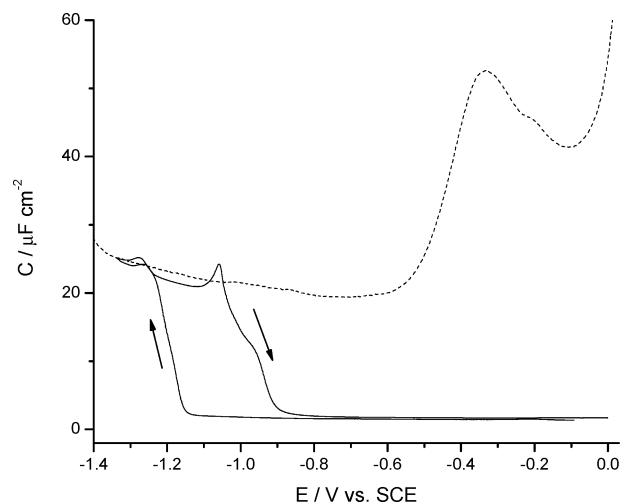


Figure 2. Differential capacity versus potential curves of a Au(111) electrode in 0.1 M NaOH for the film-free surface (dashed line) and the interface covered with a monolayer of $C_{18}SH$ (solid line). Arrows indicate direction of the voltage scan corresponding to a given segment of the differential capacity curve.

It is known that octadecanol ($C_{18}OH$) forms stable monolayers at the air/water interface that can be compressed and transferred to a solid substrate at surface pressures above 40 mN m^{-1} .^{26,30} In contrast, the $C_{18}SH$ monolayer cannot be compressed to pressures higher than 20 mN m^{-1} because the polarity of the thiol group is low and, hence, its affinity for the water subphase is low as well. Such films collapse easily. Several attempts were made to spread $C_{18}SH$ onto a 0.1 M NaOH subphase. However, compression isotherms gave molecular areas $\sim 15 \text{ \AA}^2$, indicating dissolution of the deprotonated $C_{18}S^-$ molecule into the subphase. Therefore, the transfer of the monolayer from the air/solution to the metal/solution interface had to be done on a neutral subphase and surface pressures of less than 20 mN m^{-1} . Transfers at surface pressures between 12 and 20 mN m^{-1} gave irreproducible results with transfer ratios higher than 2. However, transfer ratio values of 1.0 ± 0.1 could be achieved at the surface pressure 10 mN m^{-1} . These were the optimal conditions used in this work. The area per molecule at this value of Π is 21 \AA^2 .

Differential Capacity Measurements. The behavior of the $C_{18}SH$ coated electrode was initially characterized with differential capacity measurements. Figure 2 shows the differential capacity curves for the Au(111) electrode recorded in 0.1 M NaOH solution in the absence (dashed line) and in the presence of a $C_{18}SH$ monolayer self-assembled on the surface (solid line).

The differential capacity curve shows that the $C_{18}SH$ monolayer is stable over a potential range from -1000 to 0 mV , attaining a minimum value of $1.5 \text{ \mu F cm}^{-2}$ in that region. At potentials more negative than -1300 mV , the film is detached from the surface and the capacity increases to a value of 25 \mu F cm^{-2} and merges with the curve corresponding to the bare gold in 0.1 M NaOH. When the direction of the voltage scan is reversed, re-adsorption of the alkane thiol molecules is observed, indicating that the molecules remain close to the electrode surface, in the desorbed state. Morin and co-workers^{31–33} demonstrated that long-chain thiolates form subsurface micellar aggregates upon reductive desorption similar to those reported by Bizzotto and

(28) Dickertmann, D.; Koppitz, F. D.; Schultze, J. W. *Electrochim. Acta* **1976**, *11*, 967.

(29) Lipkowski, J.; Stolberg, L. In *Adsorption of Molecules at Metal Electrodes*; Lipkowski, J., Ross, P. N., Eds.; VCH: New York, 1992; p 171.

(30) Zawisza, I.; Burgess, I.; Szymanski, G.; Lipkowski, J.; Majewski, J.; Satija, S. *Electrochim. Acta* **2004**, *49*, 3651–3664.

(31) Yang, D.-F.; Wilde, C. P.; Morin, M. *Langmuir* **1997**, *13*, 243–249.

(32) Yang, D.-F.; Al-Maznai, H.; Morin, M. *J. Phys. Chem. B* **1997**, *101*, 1158–1166.

(33) Yang, D.-F.; Morin, M. *J. Electroanal. Chem.* **1998**, *441*, 173–181.

Lipkowski^{34,35} for amphiphilic surfactants. The hysteresis between the negative-going and positive-going traces on the differential capacity curve show that reforming the condensed film from micellar aggregates is kinetically hindered. It should be emphasized that these curves were calculated from a single frequency experiment and they do not represent the state of adsorption equilibrium. They are used only for qualitative characterization of the film behavior.

Charge Potential Curves. Chronocoulometry was used to quantitatively describe the adsorption of C₁₈SH at the Au(111) electrode surface. The charge density data determined by this technique were used for further data analysis. In chronocoulometry, the Au(111) electrode is maintained at a particular potential E_{base} where the film is adsorbed and allowed to equilibrate for 5 min. E_{base} is usually determined with the help of the differential capacity curve, and for these experiments it was set to -800 mV. After this time, the potential is stepped to an adsorption potential, E_a , and the electrode is again allowed to equilibrate for 5 min. Finally, the potential is stepped to E_{des} . The current transient due to the desorption of the thiol molecules and to the recharging of the double layer is thus measured and subsequently integrated to determine the difference between the charge density on the electrode surface at potentials E_a and E_{des} : $\Delta\sigma_M = \sigma_M(E_a) - \sigma_M(E_{\text{des}})$. $E_{\text{des}} = -1400$ mV corresponds to the potential where the film is desorbed from the surface as determined from the differential capacity curve. This procedure was repeated by varying the potential E_a between -1350 and 200 mV in 25 or 50 mV increments. Because the film is allowed to equilibrate at the base potential for 5 min to recover from the desorption step, we can reasonably assume that the film has the same initial conditions for each adsorption potential.

In order to determine the absolute charge densities, $\sigma_M(E_a)$, the following additional experiments were required. The chronocoulometric measurements were performed for the thiol-free Au(111) electrode in a nonadsorbing electrolyte (such as KClO₄).³⁶ For this electrolyte, the pzc was determined from the position of the diffuse layer minimum on the differential capacity curve recorded in a 5 mM KClO₄ solution to be 270 mV versus SCE. The absolute charge at the electrode surface was then calculated from the measured difference of charge densities at potentials E and the pzc as described in refs 27 and 29.

Next, similar measurements were performed for the thiol-free Au(111) electrode in 0.1 M NaOH solution. Chen et al. showed that at $E < -0.5$ V the OH⁻ is totally desorbed from the Au(111) electrode surface.³⁶ It is therefore reasonable to assume that at $E < -0.5$ V the absolute charge densities at the Au(111) surface are identical in 0.1 M NaOH and 0.1 M KClO₄ solutions. The absolute charge densities at the Au(111) electrode surface in 0.1 M NaOH solution were then determined from the difference between charge densities at a given potential E and charge density at $E = -0.8$ V known for the 0.1 M KClO₄ electrolyte.

Finally, the absolute charge densities for the gold electrode covered by the film of C₁₈SH were calculated assuming that the charge density at the electrode initially covered by the film is equal to the charge density measured in the absence of the film at E_{des} . This assumption is supported by Figure 2, which shows that the differential capacity of the electrode initially covered by the film merges with the capacity of the film free electrode at these negative potentials. Further, spectroscopic experiments by Bizzotto et al. demonstrated that the film of an insoluble

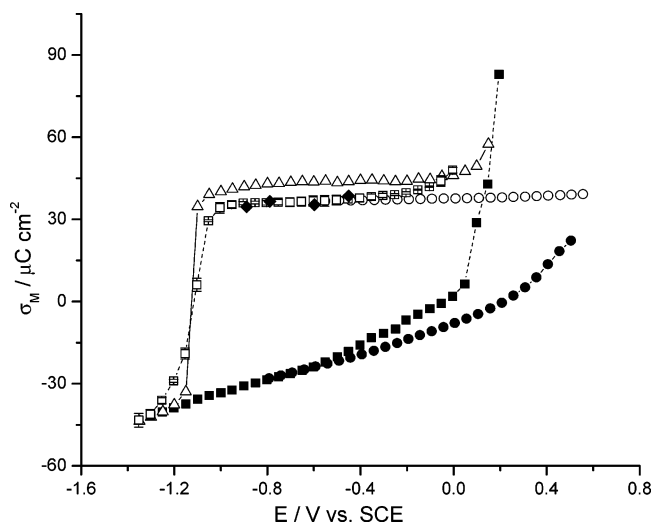


Figure 3. Charge density, σ_M , versus potential curves for the Au(111) bare electrode in 0.1 M NaOH (filled squares) and 0.1 M KClO₄ (filled circles) and with C₁₈SH adsorbed on the surface by self-assembly for 24 h (empty triangles) or LB transfer at 10 mN m⁻¹ (empty squares). Empty circles correspond to the charge densities of the LB film in 0.1 M KClO₄ as determined by stepping the potential from -0.6 V to a variable, more positive value of E . Filled diamonds show the charge density values for freshly prepared LB films.

surfactant^{34,35} or a thiol³⁷ desorbs at negative potentials but remains near the electrode surface in the form of aggregates such as micelles or flakes. Subsequent neutron reflectivity measurements by Burgess et al.^{38,39} showed that these aggregates are separated from the electrode surface by a thin ~ 1 nm thick cushion of the electrolyte.

Figure 3 shows the charge potential plots determined from the chronocoulometric experiments. It can be seen that at very negative potentials the charge density curves for the C₁₈SH-covered electrode merge with the curve of the film-free electrode, indicating that the film is totally desorbed from the gold surface. As the potential is moved in the positive direction, a large step corresponding to the adsorption of the thiol can be seen. The step for the SAM is slightly larger than for the LB film, indicating that the self-assembled film is somewhat more compact. For the electrode covered by the thiol, the curves plateau at about -1 V. However, the curve corresponding to the LB monolayer shows that the charge density starts to increase at potentials at which the onset of OH⁻ adsorption is observed for the film free electrode in 0.1 M NaOH (i.e., $\sim E > -0.4$ V). Therefore, this increase is most likely due to the onset of competitive adsorption with OH⁻ and displacement of the thiol by OH⁻ in the LB film. Such behavior occurs at more positive potentials in the case of the SAM due to the fact that the SAM is more tightly packed than the LB film.

Open circles in Figure 3 plot charge densities of the LB film in the 0.1 M KClO₄ solution. In this electrolyte, desorption of the film overlaps with the hydrogen evolution reaction and the charge due to the film desorption cannot be measured directly. However, it is reasonable to assume that at -0.6 V the charge density at the LB film-covered electrode should be the same in 0.1 M NaOH and 0.1 M KClO₄ solutions. Therefore, this plot was determined by stepping the potential from -0.6 V to a variable

(37) Shepherd, J. L.; Kell, A.; Chung, E.; Sindor, W.; Workentin, M. S.; Bizzotto, D. *J. Am. Chem. Soc.* **2004**, *126*, 8329–8335.

(38) Burgess, I.; Zamylny, V.; Szymanski, G.; Schwan, A. L.; Faragher, R. J.; Lipkowski, J.; Mejewski, J.; Satija, S. *J. Electroanal. Chem.* **2003**, *550*, 187–199.

(39) Burgess, I.; Szymanski, G.; Li, M.; Horswell, S.; Lipkowski, J.; Mejewski, J.; Satija, S. *Biophys. J.* **2004**, *86*, 1763–1776.

(34) Bizzotto, D.; Lipkowski, J. *J. Electroanal. Chem.* **1996**, *409*, 33–43.

(35) Bizzotto, D.; Lipkowski, J. *Prog. Surf. Sci.* **1995**, *50*, 237–246.

(36) Chen, A.; Lipkowski, J. *J. Phys. Chem. B* **1999**, *103*, 682–691.

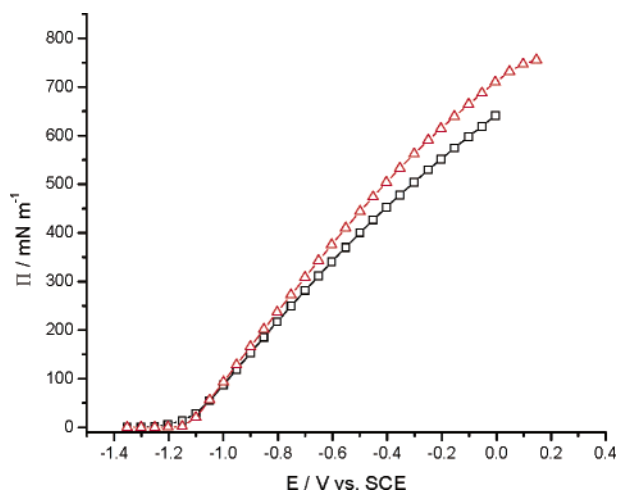


Figure 4. Surface pressure versus potential plots calculated from the charge density curves for the SAM (triangles) and the LB-transferred film (squares), 0.1 M NaOH supporting electrolyte.

more positive value of E , and the corresponding difference between the charge densities was measured. The absolute value of the charge density was then calculated by taking σ_M at $E = -0.6$ V determined earlier in 0.1 M NaOH solution. We would like to emphasize that the thiol deprotonation, which accompanies the chemisorption of thiol, took place in the Langmuir trough during the LB transfer. In 0.1 M KClO_4 , the film has never been desorbed. Even in this neutral electrolyte, the desorption takes place at a much more negative potential.

To verify that no material was lost at the desorption potential and that the readsorption of the desorbed layer was complete, additional experiments for a few selected potentials were performed using freshly transferred LB films that were desorbed only once. The data points corresponding to these measurements are marked as black diamonds in Figure 3. The agreement between charge densities determined from multiple desorption and readsorption steps and from the single desorption experiments is very good.

By integrating the area between the charge density curves for the film-free and the C_{18}SH -covered electrode, the surface pressure of the adsorbed films can be determined.^{27,29} Figure 4 shows the surface pressure plots as a function of the applied potential for the SAM and the LB films in 0.1 M NaOH electrolyte. The surface pressure of the monolayer at the metal|solution interface (~ 700 mN m^{-1}) is almost 2 orders of magnitude larger than that at the air/solution interface (10 mN m^{-1}). This huge increase in the surface pressure results from the formation of a chemisorption bond between the gold and the thiol group and should not be misconstrued as evidence that the packing densities at the A/S and M/S interfaces are fundamentally different.

Charge Numbers Per Adsorbed Molecule and Packing Density in the SAM. Figure 5 plots the difference between charge density corresponding to the film-free electrode and the charge density for the electrode covered by the SAM (triangles) and the LB transferred monolayer: (squares) in 0.1 M NaOH and (circles) in 0.1 M KClO_4 . These curves display the change in charge density of the electrode due to the adsorption of the thiol. The fact that the sign is positive indicates that a positive charge is flowing to the electrode when the C_{18}SH molecules adsorb on the gold surface. The plots have a maximum at ~ -1000 mV. For the LB films, the values of $\Delta\sigma_M$ can be used to calculate the charge number, l , with the help of eq 7. The LB films were transferred (with a transfer ratio of 1.0 ± 0.1) onto the electrode surface from the air/solution interface at a film pressure of 10

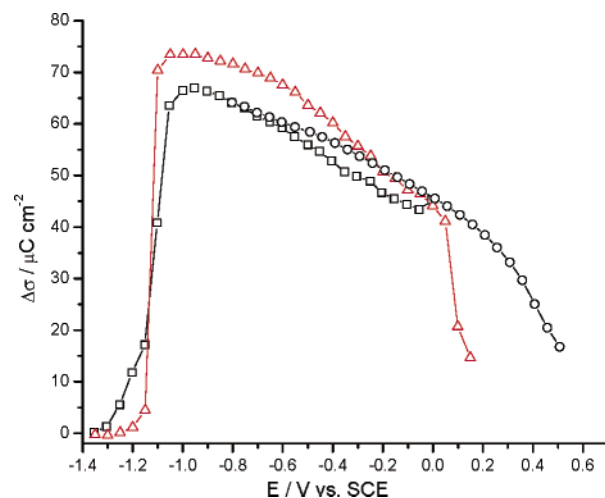


Figure 5. Charge density difference, $\Delta\sigma$, versus potential curves for the Au(111) electrode: covered by the self-assembled (triangles) and LB-transferred (squares) C_{18}SH film in 0.1 M NaOH. Open circles, $\Delta\sigma$ plot for LB film in 0.1 M KClO_4 .

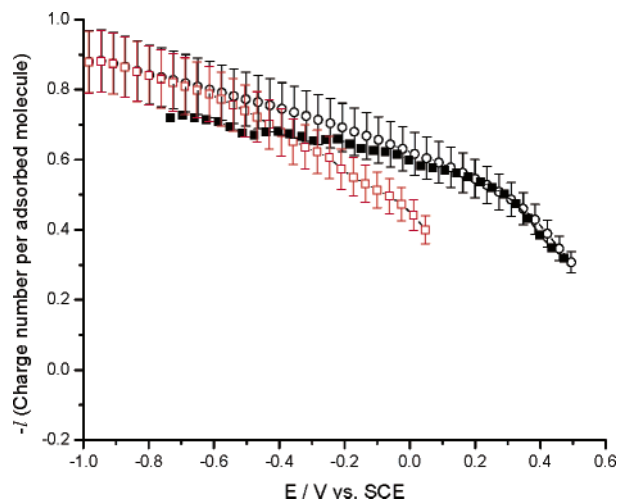


Figure 6. Charge number per adsorbed molecule for the C_{18}SH LB monolayer transferred at a surface pressure of 10 mN m^{-1} corresponding to a molecular area of 21 \AA^2 , in 0.1 M NaOH (empty squares), 0.1 M KClO_4 (empty circles), and calculated according to eq 8 (filled squares).

mN m^{-1} , which corresponds to an area per molecule of 21 \AA^2 . Within potentials corresponding to the plateau on the charge density versus E plot, we can safely state that the packing density of C_{18}SH at the metal surface was $\Gamma = 7.9 \pm 0.8 \times 10^{-10}$ mol cm^{-2} .

Figure 6 plots charge numbers calculated with the help of eq 7 and the data shown in Figure 5 as a function of the electrode potential for LB films in 0.1 M NaOH and 0.1 M KClO_4 solutions. Clearly, the charge numbers depend on the electrode potential. At the negative limit of potentials, the charge numbers approach -1 , and hence, $|l| \approx n$. However, with progressively more positive potential, $|l|$ becomes much less than unity and decreases to a value ~ 0.3 at the most positive potentials. Due to the onset of OH^- adsorption and gold oxidation, it was impossible to determine charge numbers for more positive potentials. However, it is easy to envisage that their numbers should drop to zero. This should be observed at the potential at which the charge density plot for the thiol-covered electrode intersects the charge density curve for the supporting electrolyte. This is a very significant result because it shows unequivocally that $|l|$ is not an integer but a potential-dependent parameter.

For the nonadsorbing electrolyte (0.1 M KClO₄), the dependence of l on potential can be described by the following equation:¹

$$l = -\frac{1}{F} \left(\frac{\partial \Pi}{\Gamma_{RS} \partial (E - E_{pzc}^0)} \right)_{\Gamma} = \frac{(C_0 - C_1)}{F \Gamma_{RS}} (E - E_{pzc}^0) - \frac{C_1 E_N}{F \Gamma_{RS}} - n \quad (8)$$

where Γ is the surface concentration of the adsorbed thiol, C_1 is the capacitance of the film-covered electrode, $E_{pzc}^0 = 270$ mV is the pzc of the film free electrode, E_N is the difference between the pzc of the covered and film-free electrode defined as $E_N = E_{pzc}^1 - E_{pzc}^0$, and C_0 corresponds to the capacitance as a function of potential of the bare electrode as determined from differentiating the charge density data of the film free Au(111) surface. Equation 8 was derived assuming that the desorption of the thiol is a solvent substitution reaction as described by eq 6. The full derivation and interpretation of eq 8 is given in ref 1. It shows that the charge number, l , is not a constant number but is a function of the electrode potential. As explained in ref 1, the reason for this behavior is the presence of two driving forces contributing to the desorption of the thiol molecule. The first driving force is the transfer of n electrons (cathodic reduction) which is the last term in eq 8. The additional driving force is the work done against the energy stored by the capacitor. Less energy can be stored at the interface when the electrode is covered by a SAM than when it is covered by water. This energy loss favors displacement of SAM molecules by water. Consequently, the energy needed to desorb the thiol is less than that provided by the redox reaction FE and the effective charge number is less than the number of electrons that participated in the redox reaction, which in the present case is equal to 1. The first two terms in eq 8 represent this second driving force.

The black squares in Figure 6 plot the values of l calculated with the help of eq 8. The product $C_1 E_N$ is equal to the negative of the charge density at the gold electrode covered by the LB film at E_{pzc}^0 ,⁴⁰ and the values of C_1 and C_0 were determined by differentiation of the charge potential curves in Figure 3 and $\Gamma = 7.9 \pm 0.8 \times 10^{-10}$ mol cm⁻². The agreement between charge numbers calculated using eq 8 and experimental data is within the error bars. Therefore, the solvent-substitution model predicts the potential dependence of l . It too shows that the value of the formal charge number varies from 0 to n . This result demonstrates that the basic assumption of the reductive desorption method does not hold.

It is worth noting that at E_{pzc}^0 the first term of eq 8 is equal to zero. Further, since $C_1 E_N = -\sigma_M(E_{pzc}^0)$, eq 7 shows that the term $C_1 E_N / F \Gamma_{RS}$ is equal to l . Therefore, eq 8 predicts that $2l(E_{pzc}^0) = -n$ and $-l(E_{pzc}^0) = n/2$ is equal to 0.5 when $n = 1$ for an alkane thiol. The data in Figure 6 agrees well with this prediction. In the previous work with the dithiol,¹ we observed that the charge number $-l(E_{pzc}^0) \approx 1$. This corresponds to $n/2$ for a dithiol with $n = 2$. Thus the model that considers adsorption of the thiol to be a solvent substitution reaction predicts correctly that $|l| = n/2$ at the pzc of the bare electrode. This is an interesting point worth studying in the future.

A partial charge transfer between the adsorbed thiol and the gold surface has been postulated in a number of experimental^{22,24}

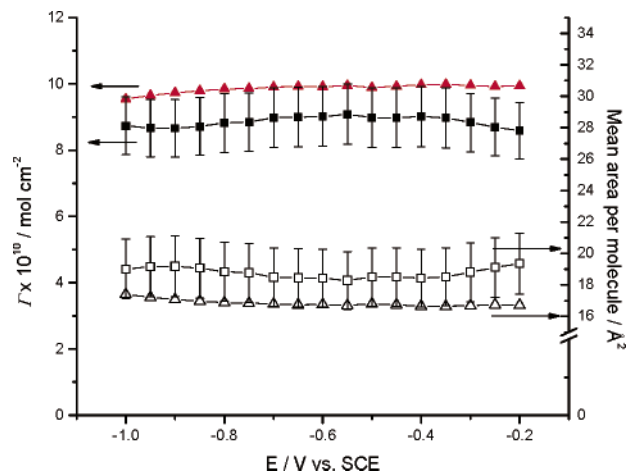


Figure 7. Surface concentration and area per molecule versus potential plots for a monolayer of C₁₈SH self-assembled at a Au-(111) surface. Squares, surface concentration (filled squares) and area per molecule (empty squares) as calculated from $\Delta\sigma$ data shown in Figure 5 and charge numbers given in Figure 6. Triangles, surface concentration (filled triangles) and area per molecule (empty triangles) as determined using the reductive desorption model and eq 9.

and theoretical studies.^{41–43} Within the experimental error of $\pm 10\%$, the present results provide no evidence that desorption of the thiol involves a partial charge transfer. A similar conclusion was reached in ref 1.

The data in Figure 6 show that the charge number $|l|$ also depends on the nature of the supporting electrolyte. At $E > -0.5$ V, the values of $|l|$ are smaller in the 0.1 M NaOH than in the 0.1 M KClO₄ solution. The differences appear at the potential corresponding to the onset of OH⁻ adsorption. Clearly, in the presence of the specific adsorption of an anion, the adsorption of the SAM involves not only solvent but also the substitution of the adsorbed anion. Therefore, the second important result of this study is to demonstrate that this substitution affects the magnitude of $|l|$.

The surface concentration and the area per molecule of the SAM can now be determined. Two contrasting approaches will be used. First, we will employ the reductive desorption method. We will then compare this result to calculated packing densities determined for the SAM using the charge numbers determined above. In order to calculate Γ using the reductive desorption method, it is convenient to write eq 3 in the following form:

$$\Gamma = \left| \frac{Q}{nF} \right| = \left| \frac{\int_{E_a}^{E_d} \frac{i}{v} dE}{nF} \right| = \left| \frac{\int_{E_a}^{E_d} C dE}{nF} \right| = \left| \frac{\sigma_M(E_d) - \sigma_M(E_a)}{nF} \right| \quad (9)$$

where $\sigma_M(E_a)$ is the charge density of the surface at a potential at which the monolayer is adsorbed and $\sigma_M(E_d)$ is the charge density at the potential at which the monolayer is desorbed. In the present case of C₁₈SH, $n = 1$ and $E_d = -1.4$ V. The charge density values needed to calculate Γ are given in Figure 3. The values of Γ determined from these data are plotted as filled triangles in Figure 7. The molecular areas that correspond to the surface concentrations are also plotted in Figure 7 as empty

(40) In principle, E_N can be determined by a linear extrapolation of the charge density plot for the monolayer covered electrode (Figure 3) to $\sigma_M = 0$ and then the product $C_1 E_N$ could be calculated. Such extrapolation is very long, and its uncertainty may be large. However, since the σ_M vs E plot is assumed to be linear and its slope is C_1 , the product $C_1 E_N$ is equal to the negative of the experimental value of σ_M for the film-covered electrode at E_{pzc}^0 ($C_1 E_N = -\sigma_M(E_{pzc}^0)$).

(41) Sellers, H.; Ulman, A.; Shnidman, Y.; Eilers, J. E. *J. Am. Chem. Soc.* **1993**, *113*, 9389–9401.

(42) Zhong, V. J.; Woods, N. T.; Dawson, G. B.; Porter, M. D. *Electrochem. Comm.* **1999**, *1*, 17–21.

(43) Zhong, C. J.; Brush, R. C.; Anderberg, J.; Porter, M. D. *Langmuir* **1999**, *15*, 518–525.

triangles. The surface concentration depends weakly on the electrode potential and is approximately equal to $10 \times 10^{-10} \text{ mol cm}^{-2}$. It corresponds to the area per molecule equal to $16.5 \pm 0.5 \text{ \AA}^2$. The minimum area of C_{18}SH calculated from the van der Waals radii is 19 \AA^2 , and several spectroscopic studies have shown that SAMs of C_{18}SH have a mean area per molecule of close to 21 \AA^2 .^{10,25,44} Therefore, the reductive desorption method gives values of coverage that are too high and areas per molecule that are physically unreasonable.

We will now use the charge numbers l (shown in Figure 6) and the $\Delta\sigma$ values for the SAM (shown in Figure 5) to determine the packing density of the SAM with the help of eq 7. Figure 5 plots $\Delta\sigma$ values corresponding to the change of the surface concentration from zero to Γ . When eq 7 is used in that case, $\Delta\Gamma = \Gamma$. The packing densities of the SAM calculated using this approach are plotted in Figure 7 (filled squares). Within the experimental error, they are independent of potential and their average value amounts to $\Gamma = 8.8 \pm 0.9 \times 10^{-10} \text{ mol cm}^{-2}$. This corresponds to an area per molecule equal to $19.0 \pm 2 \text{ \AA}^2$, as shown in Figure 7 (empty squares). This is a reasonable number in agreement with the van der Waals model, in contrast to the reductive desorption method, which gives physically unreasonable results.

We note that the coverages calculated using the reductive desorption method are too high by only 15–20%. This relatively small error explains why this method is so popular. In fact, when the double layer charging term is ignored, the reductive desorption method uses overestimated values of Q and a charge number equal to n , which is too large. Serendipitously, when the ratio of these quantities is taken, the errors partially cancel out. However, the reductive desorption method relies on assumptions and a model that are physically incorrect. The use of this method should be discouraged.

Conclusion

In this work a novel method, recently developed by Kunze et al.,¹ has been applied to measure the formal charge number per adsorbed molecule and the packing density of SAMs of C_{18}SH . We have compared packing densities determined using our new method with those obtained using the “reductive desorption” method and demonstrated that the reductive desorption method yields packing densities that are too high and therefore molecular areas that are smaller than physically possible. The results of our studies show that the reductive desorption method is systematically flawed due to errors arising from (1) failure to account for the double-layer charging contribution, (2) the misconception that the desorption process can be written as a simple reduction reaction rather than a solvent replacement reaction, and (3) incorrectly assuming that the charge flowing to the interface per desorbed molecule is an integer equal to the number of electrons transferred from the metal to the molecule. We have been able to show that the charge number per adsorbed/desorbed molecule is dependent on both the electrode potential and the nature of the supporting electrolyte. Furthermore, we have provided a physical model that explains that the potential dependence results from the fact that the cathodic desorption reaction is a substitution reaction in which water and specifically adsorbed anions compete with the thiol for adsorption sites on the electrode surface. The molecule we have chosen to study is a prototypical, alkyl chain thiol, and we feel that these results are generally applicable to all thiol-based SAMs.

Acknowledgment. This work was supported by grants from the Natural Sciences and Engineering Council of Canada and by the National Centre of Excellence in Advanced Foods and Soft Materials. J.L. acknowledges the Canada Foundation for Innovation for the Canada Research Chair Award.

(44) Chechik, V.; Schönherr, H.; Vancso, G. J.; Stirling, C. J. M. *Langmuir* **1998**, *14*, 3003–3010.